Diffusion-sensitive optical coherence tomography for real-time monitoring of mucus thinning treatments

Richard L. Blackmon,[1] Silvia M. Kreda,[2] Patrick R. Sears,[2] Lawrence E. Ostrowski,[2] David B. Hill,[1,2] Brian S. Chapman,[3] Joseph B. Tracy,[3] Amy L. Oldenburg[1]

[1]Department of Physics and Astronomy, University of North Carolina at Chapel Hill, NC 27599
[2]Marsico Lung Institute/Cystic Fibrosis Research and Treatment Center, University of North Carolina at Chapel Hill, NC 27599
[3]Department of Material Science & Engineering, North Carolina State University, Raleigh, NC 27695

Abstract

Mucus hydration (wt%) has become an increasingly useful metric in real-time assessment of respiratory health in diseases like cystic fibrosis and COPD, with higher wt% indicative of diseased states. However, available *in vivo* rheological techniques are lacking. Gold nanorods (GNRs) are attractive biological probes whose diffusion through tissue is sensitive to the correlation length of comprising biopolymers. Through employment of dynamic light scattering theory on OCT signals from GNRs, we find that weakly-constrained GNR diffusion predictably decreases with increasing wt% (more disease-like) mucus. Previously, we determined this method is robust against mucus transport on human bronchial epithelial (hBE) air-liquid interface cultures (R^2=0.976). Here we introduce diffusion-sensitive OCT (DS-OCT), where we collect M-mode image ensembles, from which we derive depth- and temporally-resolved GNR diffusion rates. DS-OCT allows for real-time monitoring of changing GNR diffusion as a result of topically applied mucus-thinning agents, enabling monitoring of the dynamics of mucus hydration never before seen. Cultured human airway epithelial cells (Calu-3 cell) with a layer of endogenous mucus were doped with topically deposited GNRs (80×22nm), and subsequently treated with hypertonic saline (HS) or isotonic saline (IS). DS-OCT provided imaging of the mucus thinning response up to a depth of 600μm with 4.65μm resolution, over a total of 8 minutes in increments of ≥3 seconds. For both IS and HS conditions, DS-OCT captured changes in the pattern of mucus hydration over time. DS-OCT opens a new window into understanding mechanisms of mucus thinning during treatment, enabling real-time efficacy feedback needed to optimize and tailor treatments for individual patients.

Keywords: polarization sensitive optical coherence tomography, gold nanorods, diffusion, diffusion sensitive optical coherence tomography

1. INTRODUCTION

The lung epithelium produces and maintains a biopolymeric mucus gel at the airway surface that is continuously cleared by airway epithelial mucociliary transport, and in humans, also by cough. In patients with cystic fibrosis (CF) and chronic obstructive pulmonary disorder (COPD), mucus becomes dehydrated, making it more viscous, inhibiting mucociliary transport. Reduction in mucociliary transport leads to chronic infection and inflammation [1, 2]. Determination of mucus rheological properties can assess the hydration state of mucus and thus yield important information for treating patients with these diseases, but current methods are limited. Particle tracking, for example, requires a stable imaging system to observe multiple micron-scale beads as they diffuse through mucus, with their mean squared displacement correlated with mucus hydration [3]. While this method has led to a better understanding of mucus rheological properties, the constraints imposed on particle tracking limit its ability to perform spatially-resolved and minimally invasive *in vivo* rheological assessment.

In comparison, employing dynamic light scattering (DLS) with OCT can provide rapid, spatially-resolved measurements of ensembles of light scatterers within each coherence volume [4]. Recently, spectral-domain OCT has been established to rapidly capture these DLS events for measuring particle diffusion [5]. We previously demonstrated that the self-diffusion rates of gold nanorods (GNR) can be obtained using polarization-sensitive, spectral-domain optical coherence

Optical Coherence Tomography and Coherence Domain Optical Methods in Biomedicine XX, edited by Joseph A. Izatt, James G. Fujimoto, Valery V. Tuchin, Proc. of SPIE Vol. 9697, 969724 · © 2016 SPIE · CCC code: 1605-7422/16/$18 · doi: 10.1117/12.2208805

tomography (PS-OCT) [6], and are sensitive to mucus concentration (% solids) [7]. Mucus is a mesh network of biopolymers with mesh pore sizes governed by mucus concentration. GNRs, PEG coated for biocompatibility, intermittently collide with these biopolymers. The rate at which the GNRs diffuse through the mesh is governed by the sizes of the mesh pores, and thus concentration of mucus. They are particularly amenable for measuring biopolymeric tissue due to their sufficiently small size (80×22 nm), making them only weakly constrained by the pores (~100s nm wide, [8]). In addition to their attractiveness as biological probes, GNRs used in this study are well suited for PS-OCT due to their optical anisotropy, with a longitudinal plasmon resonance matching the central wavelength of our system (~800 nm), resulting in a unique polarization-dependent light scattering signature easily distinguished from that of mucus. GNR diffusion rates are found by employing of DLS on co- and cross-polarized GNR backscattered light fluctuations, allowing for rapid (<0.5s) and minimally invasive assessment of mucus concentration.

Saline treatment for patients with respiratory disease has gained popularity due to its ability to safely hydrate airways and re-establish mucociliary transport [9]. For isotonic saline (IS), salt content is 0.9% and matched to the tonicity of blood and airway cells. In contrast, for hypertonic saline (HS), ionic strength is greater (7% salt concentration used in this study), and introduces an osmotic pressure gradient at the apical cell membrane. High lumenal osmolarity induces rapid changes in ion and water transport, resulting in water movement from the basolateral bath into the luminal compartment in order to equilibrate the lumenal ion concentration gradient and return to isotonicity. This is important for patients with respiratory diseases like CF, where genetic defects interrupt normal ionic channel function that results in osmotic forces that act to dehydrate mucus and create deficient mucus clearance [2, 10]. A current clinical strategy to reestablish optimal mucus hydration is the nebulization of 7% HS in CF patients [11]. Although, this treatment is effective in some patients, recent reports indicate variability in the efficacy of saline treatments across patients [12]. The variability of results in treatments indicates the need for more rigorous analysis of mechanisms at work. OCT has previously been used to study mucociliary clearance in the respiratory epithelium [13, 14] and mucus concentration [7]. In this study, we first show that the previously established correlation between GNR diffusion and mucus %solids is consistent when mucus is in motion on an actively transporting cell culture. We then use OCT time-lapse imaging to monitor culture response to IS and HS treatments. Finally, we introduce diffusion-sensitive OCT (DS-OCT) to monitor active mucus hydration to provide a measurement of therapeutic response that has never before been observed.

2. METHODS

A high-resolution, PS-OCT system previously described was used to image the samples [7]. This system consists of a Ti:Sapphire laser with a central wavelength of 800 nm, bandwidth of 120 nm, and measured axial vs. transverse resolution of 3×10 μm in water. PS-OCT applies horizontally polarized light to the sample and collects both vertical and horizontal polarization states of output light, resulting in HH (co-polarized) signals and HV (cross-polarized) signals collected simultaneously.

First, we performed an experiment to test whether the OCT-derived GNR diffusion rates are affected by mucus transport as would be present in the lung. Fully differentiated human bronchial epithelial (hBE) cells were cultured on an air-liquid interface (ALI) track model with established mucus production, mucus secretion, and mucociliary transport in order to more closely model *in vivo* airway physiology [15]. Endogenous mucus flow was verified using light microscopy prior to imaging. Pulmonary hBE cell mucus, premixed with GNRs (synthesized as previously described [16]), was topically deposited onto ALI tracks and imaged during transport in at least four different locations along the track. Spatially-averaged GNR diffusion was calculated from M-mode images (12000×4096, $t \times z$, pixels) at a linerate of 25 kHz as previously described [7].

Next, we used OCT to observe saline solution treatments on airway epithelial Calu-3 cells, which are a model of airway goblet cells [17]. Calu-3 cells express secretory mucin granules, with non-mucous cell expressing CFTR and other ion channels; these cells mimic many aspects of the airway epithelial physiology [18, 19], shown in Figure 1 below. For these studies, Calu-3 cells were cultured under ALI conditions for 10 days without washing the lumenal surface to allow for lumenal mucus accumulation. Before imaging, cells were placed in a vessel containing a HEPES-buffered HBSS-based solution (basolateral solution) and maintained at ~37ºC. B-mode OCT intensity images were collected at a rate of 25 kHz over an image size of 2000×1500 μm into 1000×1024 pixels, (transverse by axial), with a frame rate of ~0.9 Hz over a total of 9 minutes.

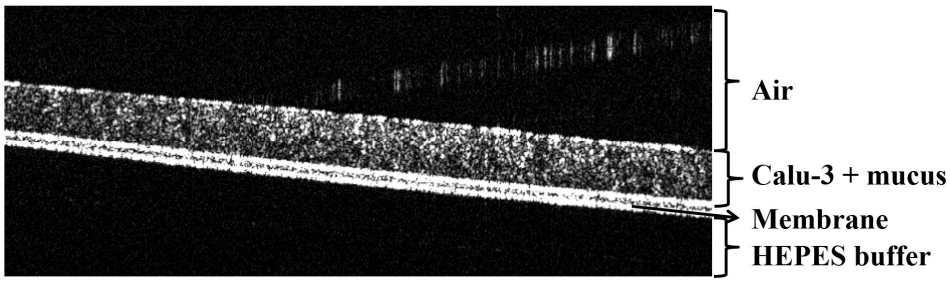

Figure 1 – B-mode OCT providing a cross-sectional view of Calu-3 cell culture used in saline treatment experiments.

Finally, DS-OCT was also used to monitor saline treatments on Calu-3 cell cultures. Calu-3 cells were cultured as above. Before imaging, 10 μL of IS containing 10^8 GNR/μL (GNR dimensions, 80×22 nm) were apically deposited and allowed to freely diffuse through native mucus >6 hours; IS is rapidly absorbed by the cells, without dilution of the mucus layer. As with B-mode OCT imaging, the cell culture was placed in a pre-warmed vessel containing HEPES-buffered HBSS-based solution. After collecting the first images, a 10 μL droplet of hypertonic saline (HS) or isotonic saline (IS), premixed with ~1% GNRs (10^8 GNR/μL), was apically deposited onto the mucus layer. The droplet was carefully deposited at a similar position in all studies, close to the culture wall. This location was chosen due to its similar proximity to the well wall for the two different cultures. The cultures were angled 10-20° in order to cause a meniscus near the well-wall after the addition of saline. DS-OCT images were constructed from depth-resolved GNR diffusion measurements. A total of 100 M-mode images (4000×4096, t×z, pixels at 25 kHz linerate) were collected in the same transverse location every 3 seconds for the first 80 s, then every 13 seconds for an additional 20 s, with imaging commencing seconds before bolus deposition, in order to capture both immediate and longer-term hydration dynamics. GNR translational diffusion rates (D_T) were calculated from the rows within each M-mode scan (z) for the ensemble of 100 M-mode scans collected over time, t. Each pixel in the DS-OCT image represents the spatially- (z) and temporally- (t) resolved D_T computed from the temporal isotropic autocorrelation (linear combination of normalized co- and cross-polarized autocorrelations as previously described [7]), $g(\tau)$, of row-wise pixel intensities, as follows:

$$g(\tau; t, z) = e^{-q^2 D_T(t,z)\tau}$$

where $q=4\pi n/\lambda_0$, $D_T(t,z)$ is the translational GNR diffusion at each depth (z), time (t) is as displayed in the diffusion map, and $g(\tau; t, z)$ represents the autocorrelation averaged over 3 M-mode image rows. DS-OCT images were 600 μm in depth and resolved to 4.65 μm after averaging over 3 rows. Corresponding cross-polarized (CP-OCT) images were constructed from the HH and HV intensities to contrast the local GNR concentration, as previously described [20].

3. RESULTS

3.1 GNR diffusion measurements are consistent in stationary and transporting mucus

Our laboratory previously established a correlation between GNR diffusion rates and the %solid concentration of mucus from normal (<~2% solid) to diseased (>~2% solid) [7]. In that study, mucus was stationary such that any movement by GNRs that contributed to signal fluctuations could be attributed to the Brownian motion of the GNRs. However, mucociliary transport during healthy respiratory function occurs at a rate of ~30-100 μm/s [21], causing a motion background to the imaging signals. To show that measurements of GNR diffusion are unaffected by this transport, we therefore conducted GNR diffusion measurements on mucus pre-mixed with GNRs and topically deposited onto actively transporting hBE cell ALI tracks. The results, shown in Figure 2, demonstrate that GNR diffusion measurements are consistent between transporting mucus and stationary mucus. This is likely due to the relatively short distance (~50 nm) mucus is transported relative to the imaging resolution (microns) over the rapid decorrelation times (<2 ms) of GNR Brownian motion. Other methods to sense mucus concentration require tracking the movement of particles over time [8]. The mean squared displacement of those particles over the time-scales observed can then be related to diffusion rates that are governed by mucus concentration. However, tracking particles over time is not only cumbersome and resource

intensive, it is limited to observations in stationary mucus and not readily translatable to measurements *in situ*. By demonstrating GNR diffusion rates are consistent in transporting mucus as with stationary mucus, we are able to move forward in monitoring mucus using GNR diffusion during treatments with the intended result of establishing mucus transport.

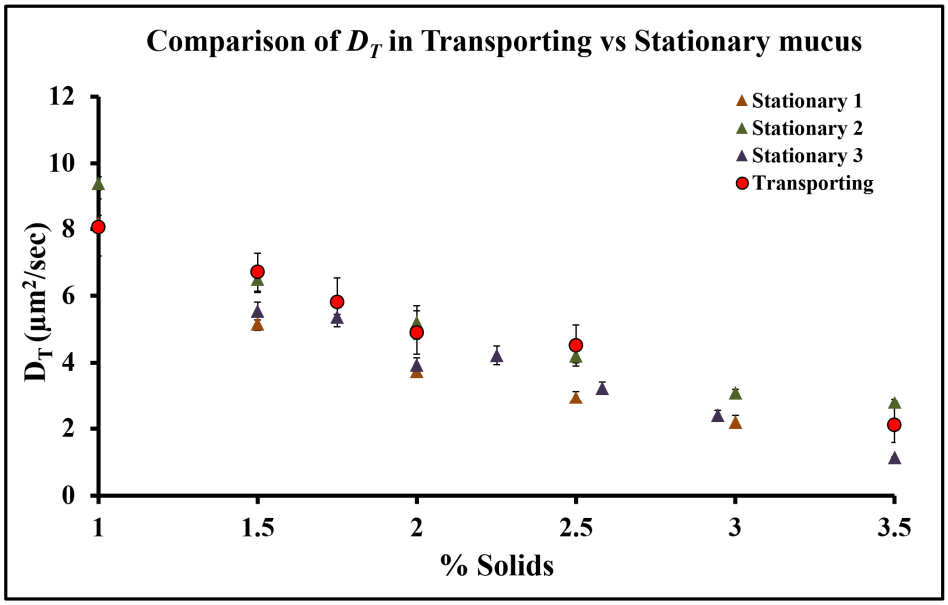

Figure 2 – Plot of GNR diffusion measurements in stationary mucus (denoted by triangular data points) and transporting mucus (denoted by circular data points). Measurements obtained at 1 % solids represent GNR diffusion in isotonic saline.

3.2 B-mode OCT images are used to monitor Calu-3 cell saline solution treatment response

We first used time-lapse B-mode OCT to visualize the effects of isotonic saline treatment on Calu-3 cell cultures; this model system has previously been used to study regulation of mucin production and drug treatments. Figure 3 shows OCT images of the cultures before, 1 minute after, and 9 minutes after treatment. Before treatment, the Calu-3 cell culture thickness (containing both cells and mucus) above the membrane (as noted in Figure 1), at the location indicated by a dotted yellow line, is ~85 μm for the culture treated with IS and ~88 μm for the culture treated with HS. The red arrow points to imaging artifacts that arise to surface reflection at a boundary normal to the imaging beam, indicating the location of the meniscus after the saline treatment. Also, the change in refractive index of the medium through which the imaging beam travels (from 1 in air to ~1.34 in saline) results in an apparent bending of the culture in the axial direction, whereas the physical geometry of the membrane is known to be flat. These two optical effects are used to determine the height of the added saline that is otherwise optically transparent.

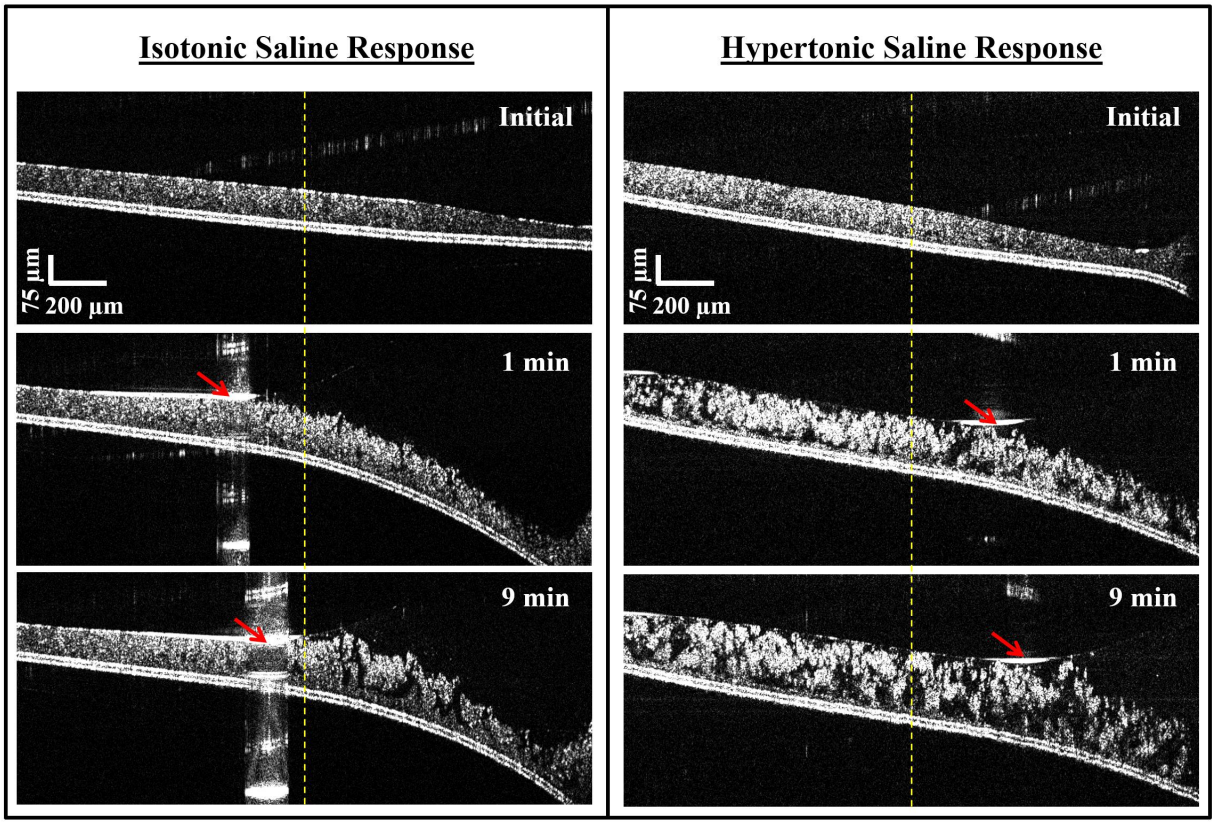

Figure 3 – B-mode OCT of IS and HS treatment response by Calu-3 cell culture, showing the initial state of the cultures pre-treament, and the state of the cultures 1 and 9 minutes post-treatment. Dotted yellow line: location of heights measured. Red arrow: Meniscus of saline.

After 1 minute of IS treatment, the mucus+cell layer at the dotted yellow line increased to ~116 µm, measured from the top of the membrane to the highest point of the swollen layer. Additionally, only the portion of the layer underneath the IS bolus (to the right of the arrow) appears to be affected by the treatment. However, for the same location after HS treatment, the layer increased to ~128 µm. Additionally, in HS-treated but not in IS-treated, areas of the mucus layer appear to be breaking away from the cell layer, as the mucus layer is "peeling off" from the cell surface. This is evidence that the increased ionic strength of the HS has introduced an osmotic pressure gradient at the cell surface, resulting in basolateral water being transported into the lumenal mucus to reach isotonicity, resulting in a net increase in the volume of the mucus layer. Interestingly, the entire layer is affected by the HS treatment, regardless of whether or not it is directly under HS.

We continued to observe the treatment response up to 9 minutes after the addition of saline. The last frames in Figure 3 show the condition of the Calu-3 cell cultures at that final time point. After the IS treatment, the thickness of the culture at the dotted line is ~132 µm. This is only a 1.5× increase over the entire 9 minute time period. The area still being actively treated by the IS (to the right of the red arrow), shows part of the layer breaking up, but to a much lesser degree than what was seen with the HS treatment. We believe this effect is primarily due to the hydration of the mucus layer that cannot be seen here with conventional OCT imaging techniques. The layer at the dotted line after 9 minutes of HS treatment, however, has increased to ~172 µm, more than double the initial height. It is important to note that the HS bolus has moved to the right of this region of interest (dotted yellow line), and that the increase in therapeutic response is occurring despite being no longer being exposed to HS. This is consistent with observations by previous investigators reporting continued mucus hydration by HS treatment for up to an hour after direct exposure [11]. In contrast, the response by IS saline appears to diminish once the saline has moved beyond that part of the layer. While OCT observation of lifting mucus from the cell layer provides useful information relevant to the re-establishment mucociliary transport, this only provides a qualitative assessment of saline treatment efficacy. Thus, without additional information

provided by DS-OCT, with conventional OCT there is no measure of the severity of mucus dehydration nor the ability to monitor hydration dynamics of mucus that could be used in quantifying treatment response.

3.3 DS-OCT quantifies hydration during mucus thinning treatments

To address the limitations of traditional OCT, we introduce DS-OCT to monitor the dynamics of mucus hydration. In DS-OCT, we quantify the GNR diffusion rate which, as shown in Fig. 2, is anti-correlated with the mucus concentration (or conversely, the mucus hydration). Figure 4 shows both DS- and CP-OCT images of Calu-3 cell response to saline treatment over time. The DS-OCT images provide an indirect measure of mucus concentration via GNR diffusion rates. Slower GNR diffusion, indicated by darker red, is a result of diffusion through more concentrated mucus that is characteristic of that seen in chronic obstructive pulmonary diseases. More rapid GNR diffusion, indicated by yellow, is a result of diffusion through thinner mucus and liquid. The CP-OCT images allow for visualization of the different layers throughout the Calu-3 cell culture. Cross-polarized signals arise from optically anisotropic scatters, like GNR-containing media. For the scale used here, this appears as yellow/green for the saline+GNRs deposited on the cultures. The cell+mucus layer and membrane layer appear as red to yellow, likely due to the lower density of GNRs in the pre-labeled mucus layer and lower cross-polarized scattering by the membrane. While all efforts were made to ensure equal densities of GNRs in the mucus layer and saline treatments, the method of topical deposition of GNRs on the mucus and pre-mixing of GNRs with saline likely introduced variability in the final GNR densities. Regions with no scatterers appear as blue (CP=0.5) due to the only intensity signals in those regions being due to noise in the system, which is relatively the same for both HH and HV OCT outputs used in calculating the CP signal.

Figure 4A shows the response to IS treatment. The distinction between the deposited IS+GNR against the endogenous mucus+cell layer is clear throughout the 8 minute viewing period, and is able to be viewed by CP-OCT. Interestingly, CP-OCT shows a mass lifting from the cell+mucus layer (purple arrow) that is likely part of the endogenous mucus layer breaking up over time, consistent with OCT time-lapse imaging. Looking at the DS-OCT image, over 8 minutes, the overall value of D_T in the top layer decreases after the initial deposit of IS (green arrow), while the overall value of D_T near the cells increases. We attribute this observation to that of the more concentrated mucus indicated by low GNR diffusion (red in DS-OCT) mixing with the liquid saline indicated by faster GNR diffusion (yellow in DS-OCT). The blending of these two layers from the initial treatment shows the hydration of mucus over time after IS treatment. While time-lapse imaging showed limited response to IS treatment, DS-OCT clearly shows a therapeutic response to the mucus layer.

Figure 4B shows the response to HS treatment. In contrast to IS, the overall value of D_T in the top layer is lower, evident by darker yellow, at the same time-points following the start of treatment (green arrow). In under a minute, GNR diffusion begins to decrease throughout the entire layer, evident by an increase in red. Lower rates of GNR diffusion indicate the presence of more concentrated mucus hindering GNR diffusion. In this way, DS-OCT shows evidence of mucus lifting from the cell layer. Additionally, as with IS, the contrast between yellow and red diminishes over time, indicating regions with faster D_T mixing with regions with lower D_T, as should be seen during active mucus hydration and swelling. Interestingly, an increasingly larger area of lower GNR diffusion appears approximately 1.5 minutes after treatment (black arrow). This suggests that mucus swelling in the y-direction may be entering the viewing plane. As with the IS condition, CP-OCT shows evidence of mucus lifting from the cell layer (purple arrow) after initial treatment. The rapid decrease in overall GNR diffusion and heterogeneous distribution of lower D_T regions is evidence of the more rapid breakdown of the mucus layer, as compared to IS treatment that is seen in Figure 3. However, at ~2.5 min, the CP-OCT signal disappears. This may be due to the reflection artifact noted by the red arrows in Figure 3. The meniscus could have moved into the imaging beam at that time-point, resulting in signal reflection from the surface rather than signal scattering from the media. But even under these non-ideal imaging conditions, DS-OCT is still able to detect some GNR diffusion that shows continued mucus hydration in the last 4 minutes of imaging. Importantly, DS-OCT analysis differentiates IS and HS treatment. In HS treatment, rapid changes in the distribution of areas with low and high restriction of GNR movement across the whole luminal layer suggest that HS initiates hydration, lifting, and mixing of the mucus layer. In contrast a similar volume of IS is not as efficient in breaking apart the dense mucus layer.

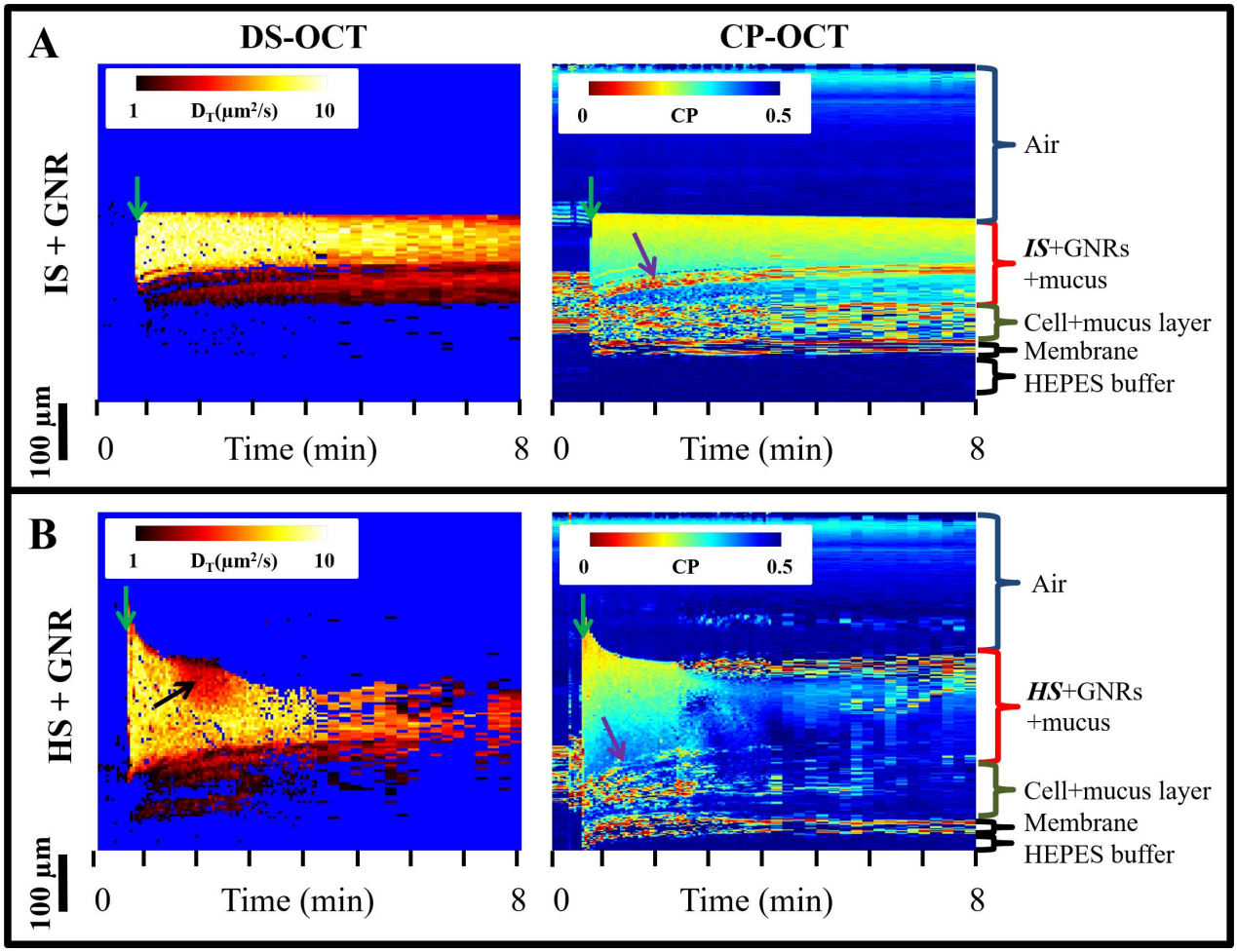

Figure 4 – Depth- and temporally-resolved DS-OCT and CP-OCT images showing the effects of (A) isotonic saline + GNR deposition and (B) hypertonic saline + GNR deposition onto Calu-3 cell culture through time. Green arrow: Initial deposition of saline treatment. Purple Arrow: CP signal presenting evidence of mucus+GNR lifting from the cell layer.

4. CONCLUSION

Treatment of respiratory diseases like CF and COPD has been hampered by an inability to study mucus thinning *in vivo* and in real-time. DS-OCT provides a novel and unique tool to quantitatively monitor the hydration of mucus for both scientific study and clinical therapeutics. Here, we have shown the result of hypertonic and isotonic saline treatments *in vitro* using time-lapse OCT imaging. We also demonstrate the ability for DS-OCT to image the dynamics of mucus hydration during two types of saline treatments clinically used. We believe DS-OCT provides a relevant tool needed to disentangle mechanisms of mucus thinning that are not fully understood in current treatments, leading to advancements in available treatments and to more personalized therapies in the clinic.

5. ACKNOWLEDGEMENTS

We acknowledge the assistance of Timothy O'Brien in the Computer Integrated Systems for Microscopy and Manipulation at the University of North Carolina at Chapel Hill and the use of the Analytical Instrumentation Facility (AIF) at North Carolina State University, which is supported by the State of North Carolina and the National Science

Foundation. This work was supported by funds from the National Institutes of Health (R21 HL 130901 and R01 HL 123557, Oldenburg, PI), (5 P01 HL 108808 and 2P30DK065988, Hill), (R01HL117836, P30DK065988, UL1RR025747; Ostrowski), and (NHLBI UH2 HL 123645 and NIDDK DK065988, Kreda), the Cystic Fibrosis Foundation (KREDA01I0, and R026-CR07/11; Kreda; KESIME14XX0, Ostrowski; and BOUCHE15R0; Kreda, Hill, and Ostrowski), the National Science Foundation (DMR-1056653; Tracy and DMS-1462992, DMS-110281; Hill), and the National Science Foundation Research Triangle Materials Research Science and Engineering Center (DMR-1121107, Tracy).

REFERENCES

[1] R. C. Boucher, "Cystic fibrosis: a disease of vulnerability to airway surface dehydration," Trends Mol Med, 13(6), 231-40 (2007).

[2] J. B. Lyczak, C. L. Cannon, and G. B. Pier, "Lung Infections Associated with Cystic Fibrosis," Clinical Microbiology Reviews, 15(2), 194-222 (2002).

[3] D. B. Hill, P. A. Vasquez, J. Mellnik *et al.*, "A biophysical basis for mucus solids concentration as a candidate biomarker for airways disease," PLoS One, 9(2), e87681 (2014).

[4] D. A. Boas, K. K. Bizheva, and A. M. Siegel, "Using dynamic low-coherence interferometry to image Brownian motion within highly scattering media," Optics Letters, 23(5), 319-321 (1998).

[5] J. Kalkman, R. Sprik, and T. G. van Leeuwen, "Path-Length-Resolved Diffusive Particle Dynamics in Spectral-Domain Optical Coherence Tomography," Physical Review Letters, 105(19), 4 (2010).

[6] R. K. Chhetri, K. A. Kozek, A. C. Johnston-Peck *et al.*, "Imaging three-dimensional rotational diffusion of plasmon resonant gold nanorods using polarization-sensitive optical coherence tomography," Physical Review E, 83(4), (2011).

[7] R. K. Chhetri, R. L. Blackmon, W. C. Wu *et al.*, "Probing biological nanotopology via diffusion of weakly constrained plasmonic nanorods with optical coherence tomography," Proc Natl Acad Sci U S A, 111(41), E4289-97 (2014).

[8] H. Matsui, V. E. Wagner, D. B. Hill *et al.*, "A physical linkage between cystic fibrosis airway surface dehydration and Pseudomonas aeruginosa biofilms," Proc Natl Acad Sci U S A, 103(48), 18131-6 (2006).

[9] C. H. Kim, M. Hyun Song, Y. Eun Ahn *et al.*, "Effect of hypo-, iso- and hypertonic saline irrigation on secretory mucins and morphology of cultured human nasal epithelial cells," Acta Otolaryngol, 125(12), 1296-300 (2005).

[10] B. Button, L.-H. Cai, C. Ehre *et al.*, "A Periciliary Brush Promotes the Lung Health by Separating the Mucus Layer from Airway Epithelia," Science, 337(6097), 937-941 (2012).

[11] S. H. Donaldson, W. D. Bennett, K. L. Zeman *et al.*, "Mucus clearance and lung function in cystic fibrosis with hypertonic saline," New England Journal of Medicine, 354(3), 241-250 (2006).

[12] V. L. Yap, and M. L. Metersky, "New therapeutic options for noncystic fibrosis bronchiectasis," Current Opinion in Infectious Diseases, 28(2), 171-176 (2015).

[13] A. L. Oldenburg, R. K. Chhetri, D. B. Hill *et al.*, "Monitoring airway mucus flow and ciliary activity with optical coherence tomography," Biomedical Optics Express, 3(9), 1978-1992 (2012).

[14] L. Liu, K. K. Chu, G. H. Houser *et al.*, "Method for Quantitative Study of Airway Functional Microanatomy Using Micro-Optical Coherence Tomography," PLoS ONE, 8(1), e54473 (2013).

[15] P. R. Sears, W.-N. Yin, and L. E. Ostrowski, "Continuous mucociliary transport by primary human airway epithelial cells in vitro," American journal of physiology. Lung cellular and molecular physiology, 309(2), L99-L108 (2015).

[16] K. A. Kozek, K. M. Kozek, W. C. Wu *et al.*, "Large-Scale Synthesis of Gold Nanorods through Continuous Secondary Growth," Chem Mater, 25(22), (2013).

[17] S. M. Kreda, S. F. Okada, C. A. van Heusden *et al.*, "Coordinated release of nucleotides and mucin from human airway epithelial Calu-3 cells," Journal of Physiology-London, 584(1), 245-259 (2007).

[18] S. M. Kreda, L. Seminario-Vidal, C. A. van Heusden *et al.*, "Receptor-promoted exocytosis of airway epithelial mucin granules containing a spectrum of adenine nucleotides," Journal of Physiology-London, 588(12), 2255-2267 (2010).

[19] B. R. Grubb, W. K. O'Neal, L. E. Ostrowski *et al.*, "Transgenic hCFTR expression fails to correct beta-ENaC mouse lung disease," American Journal of Physiology-Lung Cellular and Molecular Physiology, 302(2), L238-L247 (2012).

[20] A. L. Oldenburg, R. K. Chhetri, J. M. Cooper *et al.*, "Motility-, autocorrelation-, and polarization-sensitive optical coherence tomography discriminates cells and gold nanorods within 3D tissue cultures," Opt Lett, 38(15), 2923-6 (2013).
[21] J. W. Wong, T. G. Keens, E. M. Wannamaker *et al.*, "Effects of gravity on tracheal mucus transport rates in normal subjects and in patients with cystic-fibrosis," Pediatrics, 60(2), 146-152 (1977).